ARTICLE

OBC
www.rsc.org/obc

Arylethynylacridines: electrochemiluminescence and photophysical properties†‡

Arumugasamy Elangovan, Hsing-Hua Chiu, Shu-Wen Yang and Tong-Ing Ho*
Department of Chemistry, National Taiwan University, Taipei 106, Taiwan.
E-mail: hall@ntu.edu.tw; Fax: +886-2-2363-6359; Tel: +886-2-2369-1801

Received 16th July 2004, Accepted 8th September 2004
First published as an Advance Article on the web 30th September 2004

Electrogenerated chemiluminescence (ECL) of six new ethyne-based acridine derivatives (**1**–**6**) has been studied. The new acridine derivatives were synthesized by cross-coupling of 9-chloroacridine and corresponding donor-substituted phenylethynes under modified Sonogashira conditions. The donor groups were varied in the order of increasing steric hindrance and donor strength at the donor site. The solution phase photophysical properties and ECL of these compounds were studied comparatively in acetonitrile solvent. The UV-Visible spectra of compounds **1**–**5** exhibit closely the same maxima. Density functional theory (DFT) has been invoked to analyze and understand the unexpected UV-Visible absorption behavior. Compounds with weak electron donors produce excimer ECL irrespective of steric hindrance at the donor site, while the compound with a stronger donor gives rise to ECL that is blue-shifted with respect to its photoluminescence spectrum. All except one of these compounds also exhibit solid state fluorescence which may be useful for solid state devices such as organic light emitting diodes (OLEDs) and as laser dyes. The observed properties are discussed with reference to the structure of the compounds synthesized.

Introduction

Emission of light by recombination of charged radical ions which are generated by electrolysis of organic molecules having redox centers is called electrogenerated chemiluminescence (or electrochemiluminescence, ECL).[1] By sweeping of negative and positive potentials in sequential cycles with short time intervals, the excited states of electroactive species are made to populate the emitting state which subsequently attains the ground state emitting light of appropriate wavelength. As for the mechanism, either a singlet or a triplet state of the electroactive species can be formed depending on the annihilation enthalpy change (ΔH^0) during the electron transfer reaction. The ion annihilation can generate the singlet state (S-route)[2] if the magnitude of ΔH^0 is sufficiently larger than the energy needed for the excited singlet state (S_1). On the other hand, if the ΔH^0 is lower than S_1, but it is sufficient to generate the triplet state, then the electron transfer reaction will lead to the formation of the triplet state.[2b] However, it is yet possible to achieve singlet state by triplet–triplet annihilation, and this is known as a T-route.[2b] As a result, the light emitted from the electrochemically generated excited state of the electroactive species normally is fluorescence. ECL has been widely applied as a sensitive and selective detecting technique for many analytical applications.[2f] It has also been used as an excellent model for investigating the electron transfer mechanism.[2d] Unlike fluorescence, which requires a light source in order to excite molecules, ECL does not require a light source for excitation and hence is considered superior to fluorescence techniques in certain analytical studies.[1c] While many molecules have been known to exhibit ECL activity, most requiring amines as co-reactants, simple integral molecules emitting ECL, especially without the use of any co-reactant, are of interest to us.

Acridine is structurally similar to anthracene but possesses a nitrogen heteroatom in its central ring. However, although its homocyclic analog derivatives such as rubrene, 9-phenylanthracene and 9,10-diphenylanthracene, have been well studied and used in ECL,[3] there are no reports of acridine based bipolar molecules for luminescent, especially ECL studies and applications though there is a report on the use of acridine in mixed systems with polynuclear hydrocarbons.[4] This poor attention may be due to the high reduction potential of acridine itself [$E_{1/2}(1) = -1.62$ V and $E_{1/2}(2) = -2.38$ V].[5] The photophysics of acridine and its derivatives have recently been well studied theoretically and experimentally.[6] Exploitation of the electron transfer process in long distances in biological systems such as proteins and DNA has received much attention.[7] Several fluorophores including pyrene, 9-aminoacridine and their alkyl chain-tethered derivatives have been among the well known intercalators.[8] Further, detection of anions by acridine based bis-tren [tren = tris(2-aminoethyl)amine], the macrobicyclic tris-acridine cryptand, was studied in water through enhancement of fluorescence upon complexation.[9] In addition, acridine has been incorporated as an integral part of certain polyimdes which were applied as emissive layers and/or hole transport layers in the fabrication of light emitting devices (LED) due to their higher thermal stability caused by acridine units.[10] Acridine is of interest to us because of its ability to intercalate into/bind with many biologically important molecular fragments and report information about the host.

Structural modification in the acridine ring, especially extension of π-conjugation and introduction of electron push–pull action, would bring about changes in the properties of acridine, such as redox behavior and visible light photophysics, conducive for electro- and photoanalyses.

We have been involved in the design, synthesis and study of the ECL properties of novel ethyne based donor–acceptor systems.[11] Pursuant to our persistent endeavor of finding new molecules for ECL and LED, we have now chosen acridine as an electron acceptor unit in the new systems and varied the electron donors linked by a C–C triple bond in the order of increasing steric hindrance and donor strength. This attempt is more appropriate in the light of our recent observation that weaker donor cause excimer ECL and stronger donors cause ICT ECL in the ethyne based quinoline systems.[11a] We would like to probe the validity of the theory by the introduction of more steric hindrance at the donor site. The structures of the molecules synthesized for the present study are shown in Scheme 1.

† Electronic supplementary information (ESI) available: ^{1}H- and ^{13}C NMR and ECL spectra, and HOMO and LUMO surfaces of all compounds, and crystal structure and crystallographic details, including bond lengths and angles, for compound **6**. See http://www.rsc.org/suppdata/ob/b4/b410829a/

‡ CCDC reference number 244931. See http://www.rsc.org/suppdata/ob/b4/b410829a/ for crystallographic data for compound **6** in .cif or other electronic format.

DOI: 10.1039/b410829a

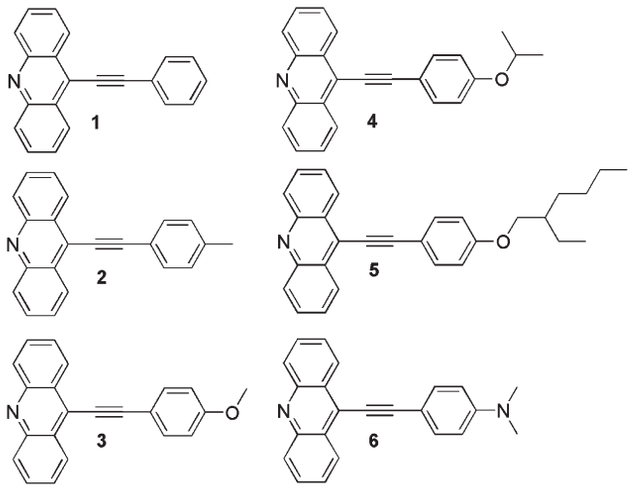

Scheme 1 Structures of phenylethynylacridines prepared and used in the present study.

Experimental

All the chemicals and reagents were purchased from Acros Organics, unless specified otherwise, and were used as received. Dichlorobis(triphenylphosphine)palladium(II) was either prepared in-house or from commercial source (Acros). 9-Chloroacridine was prepared from *N*-phenylanthranilic acid and phosphoryl chloride according to the reported method.[12] Solvents were distilled as per the standard methods and purged with argon before use. Triethylamine (TEA) and tetrahydrofuran (THF) were distilled and purged with a mixture of approximately 1 : 1 argon and hydrogen before use. ^{1}H-NMR spectra of the samples were recorded with a 400 MHz Varian instrument and ^{13}C-NMR spectra were recorded with the same instrument at 100.1 MHz operator frequency in $CDCl_3$ solvent (Merck) with $CHCl_3$ internal standard (δ 7.24 ppm for ^{1}H and 77 ppm, middle of the three peaks, for ^{13}C spectra. Mass spectra were recorded with a JEOL SX 102A instrument on a nitrobenzyl alcohol matrix. TLC was run on Merck precoated aluminium plates (Si 60 F_{254}). Column chromatography was run on Merck silica gel (60–120 mesh) or neutral alumina (Merck) 70–230 mesh.

All UV-Visible spectra were recorded on a HITACHI U-2000 spectrophotometer with 10 μM solution of the compounds in CH_3CN and all fluorescence spectra on a HITACHI F-3010 fluorescence spectrophotometer using similar solution concentrations. Fluorescence quantum yields (Φ) were determined in CH_2Cl_2 with reference to coumarin 1 standard (Φ = 0.5 in MeOH).[13] CV measurements were done on a CH Instruments Electrochemical Analyzer. The cell used is a three-electrode cell consisting of a carbon disc (2.0 mm) working electrode, a platinum wire counter electrode and a Ag/AgCl reference electrode. The scan rate was 100 mV s^{-1}. ECL spectra were recorded at room temperatures using a setup consisting of an F-3010 Fluorescence spectrophotometer, a CV-27 Voltammograph with a computer interface. The electrode surfaces were prepared freshly before CV and ECL experiments. The carbon disc electrode was rubbed against alumina paste and the Pt electrode was cleaned by rinsing with dilute nitric acid followed by water and then fired with a naked flame to ensure maximum cleanliness of the electrode. Typically a 1 mM concentration of the compound solution in degassed acetonitrile[2b] with 0.05 M tetrabutylammonium perchlorate (TBAP) was used. To generate the annihilation reaction, the platinum electrode was pulsed between the first reduction and first oxidation potentials and the pulse interval was controlled on a computer. All measurements were done at room temperature (22–23 °C).

General procedure for the synthesis of 9-*p*-tolylethynylacridine (2)

9-Chloroacridine (prepared according to ref. 12) 213.7 mg (1 mmol), $(PPh_3)_2PdCl_2$ 14 mg (2 mol%), CuI 4 mg (2%), PPh_3 26 mg (10%) and a stirring bar were charged in a two neck round-bottomed flask equipped with a condenser and the setup was degassed and back-filled three times with a gaseous mixture of Ar + H_2. THF (8–10 mL) was introduced *via* a syringe into the reaction flask followed by 6 equivalent of TEA and finally by a solution of the terminal acetylene (1.1 mmol) [4-tolylacetylene (Aldrich) 127 mg] in 5 mL THF *via* a syringe under the mild reducing atmosphere at about 60 °C. After the addition of the alkyne, the reaction mixture was refluxed for 8–10 h. When the TLC indicated disappearance of starting compounds, the volatiles were evaporated and the residue was recrystallized from toluene to get pure **2** as yellow crystals 222 mg (76%); mp: 156–158 °C; ^{1}H NMR (400 MHz, $CDCl_3$): δ 8.55 (d, *J* 8.4 Hz, 2H), 8.23 (d, *J* 8.8 Hz, 2H), 7.79 (t, *J* 7.6 Hz, 2H), 7.67 (d, *J* 8.4 Hz, 2H), 7.61 (t, *J* 7.5 Hz, 2H), 7.27 (d, *J* 7.6 Hz, 2H), 2.43 (s, 3H); ^{13}C NMR (100 MHz, $CDCl_3$): δ 148.76, 140.35, 132.29, 130.73, 130.11, 129.80, 128.66, 127.10, 126.84, 126.81, 119.70, 106.14, 84.09, 22.32; High Mass (M^+) *m*/*z*: 293.1205 calculated for $C_{22}H_{15}N$: 293.1204.

9-Phenylethynyl-acridine (1). Mp: 164–165 °C; ^{1}H NMR (400 MHz, $CDCl_3$): δ 8.55 (d, *J* 8.4 Hz, 2H), 8.24 (d, *J* 8.8 Hz, 2H), 7.79 (m, 4H), 7.62 (t, *J* 7.5 Hz, 2H), 7.46 (m, 3H); ^{13}C NMR (100 MHz, $CDCl_3$): δ 148.75, 132.32, 130.66, 130.16, 129.86, 128.99, 128.21, 126.97, 126.86, 126.82, 122.73, 105.56, 84.53; High Mass (M^+) *m*/*z*: 279.1028 calculated for $C_{21}H_{13}N$: 279.1048.

9-(4-Methoxy-phenylethynyl)-acridine (3). Mp: 167–169 °C; ^{1}H NMR (400 MHz, $CDCl_3$): δ 8.56 (d, *J* 8.8 Hz, 2H), 8.24 (d, *J* 8.8 Hz, 2H), 7.80 (t, *J* 8.6 Hz, 2H), 7.73 (d, *J* 8.8 Hz, 2H), 7.62 (t, *J* 8.6 Hz, 2H), 6.99 (d, *J* 8.8 Hz, 2H), 3.88 (s, 3H); ^{13}C NMR (100 MHz, $CDCl_3$): δ 160.89, 148.85, 133.95, 130.58, 130.19, 128.69, 127.08, 126.72, 126.64, 114.83, 114.69, 106.10, 83.68, 55.92; High Mass (M^+) *m*/*z*: 309.1148 calculated for $C_{22}H_{15}NO$: 309.1154.

9-(4-Isopropoxy-phenylethynyl)-acridine (4). Mp: 145–147 °C; ^{1}H NMR (400 MHz, $CDCl_3$): δ 8.54 (d, *J* 8.4 Hz, 2H), 8.21 (d, *J* 8.8 Hz, 2H), 7.78 (t, *J* 7.8 Hz, 2H), 7.69 (d, *J* 8.8 Hz, 2H), 7.60 (t, *J* 7.4 Hz, 2H), 6.95 (d, *J* 8.8 Hz, 2H), 4.62 (septet, *J* 6.0 Hz, 1 H), 1.37 (d, *J* 6.4 Hz, 2H); ^{13}C NMR (100 MHz, $CDCl_3$): δ 159.38, 148.85, 134.02, 130.65, 130.18, 128.88, 127.14, 126.76, 126.67, 116.31, 114.40, 106.36, 83.58, 70.59, 22.57; High Mass (M^+) *m*/*z*: 337.1471 calculated for $C_{24}H_{19}NO$: 337.1467.

9-[4-(2-Ethyl-hexyloxy)-phenylethynyl]-acridine (5). Pale liquid; ^{1}H NMR (400 MHz, $CDCl_3$): δ 8.53 (d, *J* 8.4 Hz, 2H), 8.21 (d, *J* 8.8 Hz, 2H), 7.77 (t, *J* 7.8 Hz, 2H), 7.69 (d, *J* 10.4 Hz, 2H), 7.59 (t, *J* 7.5 Hz, 2H), 6.96 (d, *J* 8.4 Hz, 2H), 3.89 (d, *J* 6.0 Hz, 2H), 1.75 (sextet, *J* 6.0 Hz, 1H), 1.46 (m, 4H), 1.32 (m, 4H), 0.91 (m, 6H); ^{13}C NMR (100 MHz, $CDCl_3$): δ 160.84, 148.87, 133.94, 130.60, 130.19, 128.86, 127.13, 126.75, 126.65, 115.28, 114.50, 106.38, 83.63, 71.22, 39.91, 31.09, 29.68, 24.46, 23.64, 14.71, 11.76; High Mass (M^+) *m*/*z*: 407.2240 calculated for $C_{29}H_{29}NO$: 407.2249.

9-[4-(*N*,*N*-Dimethylamino)-phenyl]ethynyl-acridine (6). Mp: 230–232 °C; ^{1}H NMR (400 MHz, $CDCl_3$): δ 8.56 (d, *J* 8.0 Hz, 2H), 8.20 (d, *J* 8.8 Hz, 2H), 7.77 (t, *J* 7.7 Hz, 2H), 7.64 (d, *J* 9.2 Hz, 2H), 7.58 (t, *J* 7.5 Hz, 2H), 6.72 (d, *J* 9.2 Hz, 2H), 3.04 (s, 6H); ^{13}C NMR (100 MHz, $CDCl_3$) δ 151.19, 148.94, 133.76, 130.52, 130.11, 129.60, 127.33, 126.5, 126.33, 112.16, 109.17, 108.4, 83.59, 40.68; High Mass (M^+) *m*/*z*: 322.1470 calculated for $C_{23}H_{18}N_2$: 322.1470.

Theoretical calculations

Theoretical calculations were performed using Spartan'04™ for Windows, Wavefunction Inc., Irvine, CA 92612, USA. Molecules were built and optimized at the B3LYP level of

Table 1 Photophysical data of compounds **1**–**6**

Compound	λ_{max}^{Abs}/nm, eV [ε_{max}][a]	λ_{max}^{Flu}/nm, eV	Φ^b	Stokes shift/nm	Solid state emission λ_{max}/nm
1	417, 2.97 [1.62]	431, 2.88	0.16	14	487
2	419, 2.96 [1.38]	434, 2.86	0.27	15	520
3	422, 2.94 [1.46]	464, 2.67	0.59	42	540
4	424, 2.92 [2.03]	469, 2.64	0.53	44	494
5	424, 2.92 [2.50]	466, 2.66	0.62	42	—
6	446, 2.78 [2.15]	569, 2.18	0.043	123	554

[a] ($\times 10^4$ M^{-1} cm^{-1}). [b] Fluorescence quantum yield (Φ) measured in CH_2Cl_2 with reference to coumarin 1 (Φ = 0.50 in MeOH).[13]

density functional theory (DFT) using 6-31G* basis set at ground state, and orbital energies and HOMO–LUMO energy gaps were calculated subsequently. HOMO and LUMO surfaces are provided in the Supplementary Information.†

Result and discussion

Compounds **1–6** were prepared in good yields by palladium-catalyzed Sonogashira coupling of 9-chloroacridine with donor-bearing terminal arylalkynes under a mild reducing atmosphere of hydrogen and argon according to our reported method.[14] All compounds were characterized by ^{1}H-NMR, ^{13}C-NMR and high resolution mass spectra (see Supplementary Information for spectra†).

Photophysical properties

The UV-Visible absorption spectra of all the compounds were recorded in acetonitrile solvent at room temperatures (22–23 °C). All compounds absorb moderately (*cf.* ε_{max} Table 1) and exhibit absorption maxima characteristic of a π–π* transition as the longest wavelength absorption along with a β-band absorption around 260 nm. Compounds **1**–**5** show closely similar maxima in their absorption spectra. Although Table 1 carries the maximum absorption wavelengths (and energy in eV), the onset of the maxima occur at about 440 nm (2.8 eV) (Fig. 1). Compound **6** stands out from the series by showing the longest wavelength of absorption starting at about 500 nm (2.5 eV) with a maximum at 446 nm. This is due to the efficient charge transfer caused by the introduction of a strong electron donor NMe_2 group which may increase the energy level of highest occupied molecular orbital (HOMO).

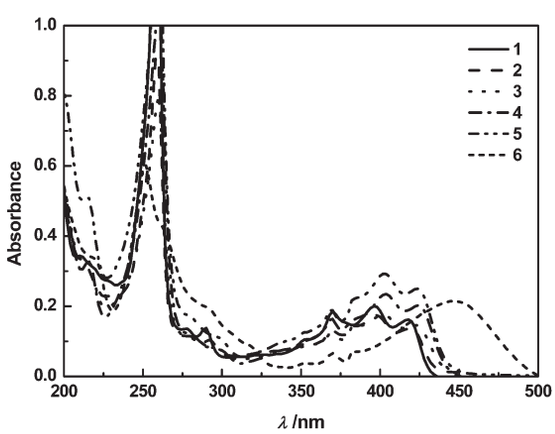

Fig. 1 UV-visible absorption spectra of **1**–**6** recorded in CH_3CN (10 μM).

The anomolous UV-Visible absorption behavior could be understood by analyzing the highest occupied molecular orbital (HOMO) and lowest unoccupied molecular orbital (LUMO) surfaces of these compounds using density functional theory. The orbital surfaces and energy levels can be compared with those of free acridine. The HOMO and LUMO for compound **1** are well delocalized throughout the molecule. Whereas for **2**–**5** both HOMO and LUMO are both localised mainly on the acridinyl moiety with extension only up to the C–C triple bond and the donor group remains cut off. This indicates that the electronic transition is vastly borne by the acridinyl moiety and hence it is observed that compounds **2**–**5** absorb at closely similar wavelengths showing structured bands. However the scene takes a dramatic twist in the case of **6** for which the HOMO is localised on the donor bearing phenyl moiety and the LUMO entirely on the acridinyl moiety (see Supplementary Information for figures†). Therefore the electronic transition in the case of **6** is from the HOMO of the donor to the LUMO of the acridine suggesting ICT. This can be seen from its structureless absorption band at the longest wavelength.

Fig. 2 shows the calculated energy level diagram for the compounds **1**–**6** and acridine. It can be seen that the LUMO energy is reduced relative to that of acridine whereas the HOMO is raised slightly for **1**–**5** and highest for **6**. The HOMO–LUMO energy gaps remain in the range of 3.14–3.36 eV for **1–6** while the gap for free acridine is 3.7 eV. The theoretical gaps are expectedly higher by 0.15–0.25 eV than the experimental values (Table 1) as the calculations were done for molecules in the gas phase. However reduction in the energy gap for **1**–**6** can be attributed to the extension of π-conjugation.

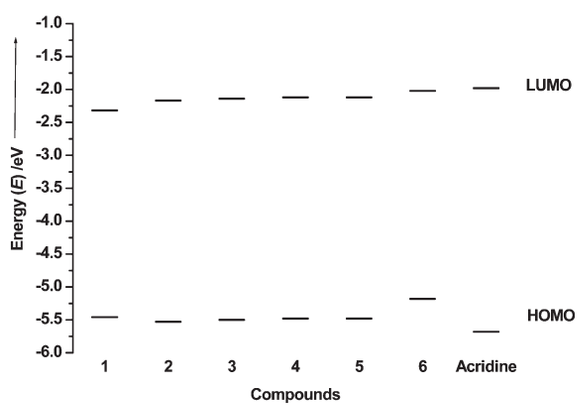

Fig. 2 Calculated HOMO–LUMO energy levels for **1**–**6** and free acridine.

All the compounds are visibly fluorescent green in methylene chloride–chloroform solutions with **6** being yellow–green fluorescent. The solution fluorescence spectra of compounds **1**–**5** were recorded in acetonitrile while that of **6** in methylene chloride as it did not show fluorescence in acetonitrile (Fig. 3). Compounds **1** and **2** show closely similar emission maxima around 430 nm with vibrational fine structure, while **3**–**5** show slightly red-shifted emission around 465 nm as a structureless band with enhanced emission quantum yields (*cf.* Φ) and the trend is also observed in the Stokes shift. For **1** and **2** there is only a marginal Stokes shift while for **3**–**5** the shift is considerably larger. Compound **6** is outstanding in its emission property as well as in that it shows a distinct broad emission maximum at 569 nm albeit with a lower quantum yield and with a Stokes shift of 123 nm. This behavior is attributed to the presence of a strong electron donating NMe_2 group which makes the molecule's energy difference between excited state geometry and ground state geometry larger. Probably this molecule undergoes torsional motion to achieve maximum twist between the donor

and acceptor moieties with respect to the C–C triple bond. The lower fluorescence quantum yield may be due to the strong intramolecular charge transfer (polar compound) which either quenches fluorescence or leads to a low lying excited state. This state of affairs is more prominent especially in highly polar acetonitrile in which no fluorescence was observed.

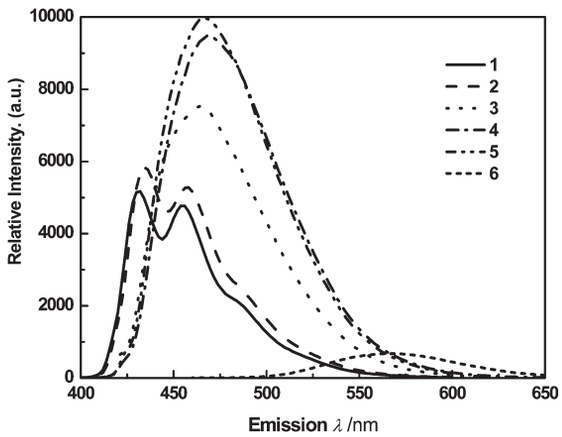

Fig. 3 Fluorescence emission spectra of **1**–**6** [**1**–**5** were recorded in CH_3CN (10 μM) and **6** in CH_2Cl_2].

Compounds **1**–**4** and **6**, which are solids, were found to emit fluorescence in the solid state upon irradiation with black light (364 nm). Hence, qualitative solid state emission spectra were recorded and are shown in Fig. 4. Compounds **1**–**3** appear to show excimer emission while **4** and **6** appear to show monomeric emission which can be compared with solution photoluminescence.

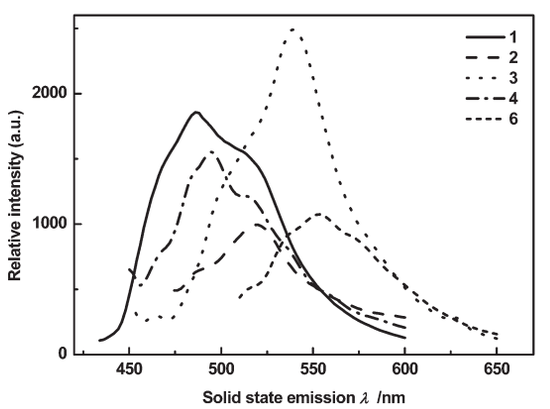

Fig. 4 Solid state fluorescence spectra of **1**–**4** and **6**.

Electrochemical analysis and ECL

Cyclic voltammetry (CV) was performed on all the compounds to determine their electroactivity and to arrive at their redox potential values before electrochemiluminescence studies. A 1 mM concentration solution of the compound in degassed acetonitrile with 50 mM TBAP was employed for the CV measurements with a 100 mV s^{-1} scan rate. All the compounds had a reversible reduction peak and an irreversible or a quasi-reversible oxidation peak. The reduction peak potential for compounds **1**–**5** occurs at about −0.85 V and the oxidation potential at about 1.5–1.6 V (Table 2). Compound **6** follows a trend observed in its photophysical properties. The CV trace of compound **6** is shown in Fig. 5; the reduction peak potential at −0.84 V can be ascribed to the reduction at the acridine moiety[5] and the oxidation peak at 0.98 V is due to the oxidation occurring at the *N*,*N*-dimethylaminophenyl group.[11c] Introduction of the strong electron donating NMe_2 group has brought down the oxidation potential. This is indicative of the reduction in the energy gap between the LUMO and HOMO in this system. This reduction in the HOMO–LUMO gap is also discernible from the photophysical properties of **6** (*vide supra*).

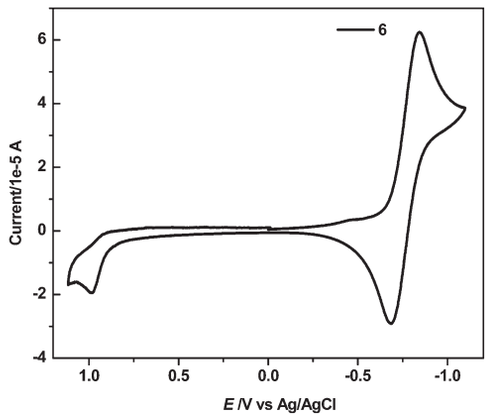

Fig. 5 Cyclic voltammogram of **6** in acetonitrile (1 mM with 50 mM TBAP. Scan rate: 100 mV s^{-1}).

In general, extension of π-conjugation has reduced the reduction potential and favored easier reduction as compared to the parent acridine.[5]

ECL spectra were recorded[11d] with a sample concentration of 1.0 mM in the presence of TBAP (50 mM) in CH_3CN. Voltage was pulsed between the first positive and first negative peak potentials with varying stepping pulse rates and intervals in order to get a optimum ECL spectra (see ESI for spectra and voltage pulse rates†). All compounds exhibited ECL with appreciable intensities relative to $Ru(bpy)_3^{2+}$. Compounds **1**–**5** show ECL with maxima red shifted in comparison with their fluorescence maxima by 20–40 nm. It may be safely ascribed to the emission from the excimer of the annihilated product responsible for ECL emission (E-route). Compound **6** can be considered as emitting ECL from an aggregate in which the acridine moiety of two molecules face each other inversely with the NMe_2 substituted phenyl donor groups projecting away from the centre (Fig. 6). This kind of structure is most likely formed at the concentration used for ECL studies which is 100 folds more concentrated than that used for fluorescence studies.

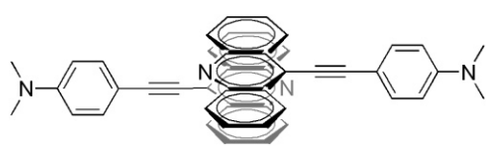

Fig. 6 Structure of aggregate formation proposed for ECL of **6**.

X-Ray crystal structure analysis of compound **6** revealed features supporting the foregoing argument.[16] The compound crystallized as a triclinic prism with two acridinyl heads invertedly facing each other with the *N*,*N*-dimethylaminophenyl groups projecting nearly perpendicularly away in opposite directions (Fig. 7) consistent with the structure depicted in Fig. 6. The dihedral angle between the plane of the acridine and that of the donor-bearing phenyl is measured to be 73.3° and the interplanar distance between the two offset parallel planes of the acridines at 91.83° was measured to be 3.59 Å. At higher concentrations under ECL measurement conditions the ECL emissive species may attain a structure as shown in Fig. 6 and hence the blue shifted ECL spectra for **6**. For comparison, the fluorescence spectrum of **6** was recorded in CH_2Cl_2 as well as at the same concentration used for ECL measurements (1 mM). We found that the photoluminescence maximum is only red shifted by about 10 nm (573 nm) as compared to that at 10 μM solution and with drastically reduced intensity (one-seventh). Therefore the ECL emissive species is believed to be unique and quite different from that of the photoluminescent species. The ECL spectra could be reproduced for 8–10 electrochemical cycles, however the intensity showed reduction upon cycling any further. A similar observation has been made in the case of *N*,*N*-dimethylaminophenyl-4-quinolinylethyne (compound **6** minus one phenyl ring in the acridine).[11c]

Table 2 Electrochemical and ECL data of **1**–**6**

Compound	λ_{max}^{ECL}/nm, eV	Relative intensity[a]	$E_{p,OX}$/V	$E_{p,RED}$/V	$-\Delta H^0$/eV[b]
1	473, 2.62	0.044	1.668	−0.867	2.375
2	482, 2.57	0.022	1.672	−0.853	2.365
3	480, 2.58	0.09	1.643	−0.805	2.288
4	487, 2.55	0.012	1.536	−0.859	2.235
5	479, 2.59	0.021	1.540	−0.864	2.244
6	534, 2.32	0.01	0.984	−0.842	1.666

[a] Relative to $Ru(bpy)_3^{2+}$ (1.0). [b] Calculated using the equation: $-\Delta H^0 = E_{p,OX} - E_{p,RED} - 0.16$ V.[15]

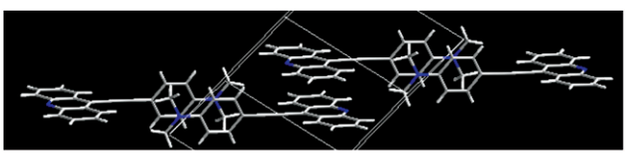

Fig. 7 X-Ray crystal packing diagram showing π-stacking interaction between the two adjacent acridinyl units. The inter-planar distance between the two planes of acridine was measured to be 3.59 Å.

Based on the foregoing arguments a probable mechanism may be proposed for the formation of an aggregate under ECL conditions as shown in Scheme 2.

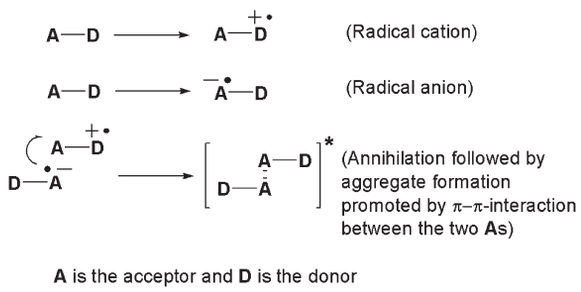

Scheme 2 Probable mechanism for the formation of an aggregate during ECL.

In order to ascertain the mechanism of ECL emission, whether it is a S-route or a T-route, the enthalpy change of radical ion annihilation reaction ($-\Delta H^0$) was calculated from the equation:[15]

$$-\Delta H^0 = E_{p,OX} - E_{p,RED} - 0.16\ \text{eV}$$

The enthalpy change values for radical ion-annihilation reactions, along with the ECL maxima are given in Table 2. The enthalpy changes of the annihilation reaction in all the cases studied here have lower values (1.7–2.4 eV) as compared to their ECL maxima (2.3–2.6 eV) and hence the annihilation reaction did not produce sufficient energy to populate the singlet exited state and therefore triplet–triplet annihilation must have occurred to provide the energy required for the formation of excited state which in turn emits ECL.

Conclusion

A new series of donor–acceptor ethynes with acridine as acceptor and several donor substituted phenyl groups have been synthesized and their ECL properties were studied. All the compounds exhibit ECL from the annihilation of the radical anions and radical cations *via* T-route. Compounds with weak donors, irrespective of whether sterically capable of causing hindrance or not, emit excimer ECL. Compounds with strong donors such as the NMe_2 group gives rise to blue shifted ECL. Further it is hereby confirmed that the excimer ECL and monomeric ECL are determined by strength of the electron donating group rather than steric hindrance at the donor site. While neither the parent acridine nor the isolated donor-substituted benzene is capable of producing ECL, it may be inferred that the extension of conjugation imparts new properties to the resultant molecules which are not commonly anticipated for the parent compounds. The observance of solid state fluorescence emission promotes more interest in these molecules for further application in solid state devices such as organic light emitting diodes and lasers. Though the ECL was studied in acetonitrile solvent, introduction of functional groups such as SO_3^- could make them water soluble and the ECL immunoassay could well be carried out in aqueous solutions. In view of the potential binding nature of the acridines to a variety of guest species, the compounds reported here and their water-soluble derivatives may find application in immunoassay and other sensing applications.

Acknowledgements

Financial support for this work was provided by the National Science Council, Taiwan. We thank Professor S. M. Peng and Mr G. S. Lee for providing X-ray data for compound **6**.

References

1 (*a*) L. R. Faulkner, and A. J. Bard, Electrogenerated Chemiluminescence, in *Electrochemical Methods*, John Wiley & Sons, New York, 1980, pp. 621–627; (*b*) A. W. Knight and G. M. Greenway, *Analyst*, 1994, **119**, 879; (*c*) A. W. Knight, *Trends Anal. Chem.*, 1999, **18**, 47; (*d*) R. Y. Lai, E. F. Fabrizio, S. A. Jenekhe and A. J. Bard, *J. Am. Chem. Soc.*, 2001, **123**, 9112; (*e*) I. Prieto, J. Teetsov, M. A. Fox, D. A. Vanden Bout and A. J. Bard, *J. Phys. Chem.*, 2001, **A105**, 520; (*f*) M. Oyama and S. Okazaki, *Anal. Chem.*, 1998, **70**, 5079; (*g*) A. Kapturkievicz, *J. Electroanal. Chem.*, 1990, **290**, 135; (*h*) A. Kapturkievicz, *J. Electroanal. Chem.*, 1991, **302**, 13.

2 (*a*) T. Kuwana, in *Electroanalytical Chemistry*, A. J. Bard, ed., Marcel Dekker, New York, 1966, vol. 1, ch. 3; (*b*) A. J. Bard and L. R. Faulkner, in *Electroanalytical Chemistry*, A. J. Bard, ed., Marcel Dekker, New York, 1977, vol. 10, p. 1; (*c*) D. M. Hercules, *Acc. Chem. Res.*, 1969, **2**, 301; (*d*) R. Y. Lai, E. F. Fabrizio, L. Lu, S. A. Jenekhe and A. J. Bard, *J. Am. Chem. Soc.*, 2001, **123**, 9112; (*e*) L. R. Faulkner and A. J. Bard, Electrogenerated Chemiluminescence, in *Electrochemical methods*, John Wiley & Sons, New York, 1980, pp. 621–627; (*f*) M. M. Richter, *Chem. Rev.*, 2004, **104**, 3003; (*g*) N. R. Armstrong, R. M. Whightman and E. M. Gross, *Annu. Rev. Phys. Chem.*, 2001, **52**, 391.

3 (*a*) D. M. Hercules, *J. Am. Chem. Soc.*, 1969, **91**, 301; (*b*) R. E. Visco and E. A. Chandross, *J. Am. Chem. Soc.*, 1964, **86**, 5350; (*c*) K. S. V. Santhanam and A. J. Bard, *J. Am. Chem. Soc.*, 1965, **87**, 139; (*d*) D. M. Hercules, *Science*, 1964, **145**, 808.

4 T. D. Santa Cruz, D. L. Akins and R. L. Birke, *J. Am. Chem. Soc.*, 1976, **98**, 1677.

5 Ref. 4 and B. J. Tabner and J. R. Yandle, *J. Chem. Soc. A*, 1968, 381.

6 (*a*) Ò. Rubio-Pons, L. Serrano-Andrés and M. Merchán, *J. Phys. Chem.*, 2001, **105**, 9664; (*b*) J. Prochorow, I. Deperasińska and O. Morawski, *J. Mol. Struct.*, 2000, **555**, 97; (*c*) P. Nikolov and H. Görner, *J. Photochem. Photobiol., A*, 1996, **101**, 137.

7 (*a*) S. A. Wallin, E. D. A. Stemp, A. M. Everest, J. M. Nocek, T. L. Netzel and B. M. Hoffman, *J. Am. Chem. Soc.*, 1991, **113**, 1842; (*b*) A. W. Axup, M. Albin, S. L. Mayo, R. J. Crutchley and H. B. Gray, *J. Am. Chem. Soc.*, 1988, **110**, 435; (*c*) D. N. Beratan and J. N. Onuchic, *Photosynth. Res.*, 1989, **22**, 173; (*d*) J. K. Barton, V. K. Challa and N. J. Turro, *J. Am. Chem. Soc.*, 1986, **108**, 6391; (*e*) N. J. Turro and J. K. Barton, *Science*, 1988, **241**, 5361; (*f*) E. D. A. Stemp, M. R. Arkin and J. K. Barton, *J. Am. Chem. Soc.*, 1995, **117**, 2375; (*g*) C. J. Murphy, M. M. Arkin, N. D. Ghatlia, S. Bossman, N. J. Turro and J. K. Barton, *Proc. Natl. Acad. Sci. USA*, 1991, **91**, 5315.

8 (*a*) A. R. Peacocke and N. J. H. Sherrett, *Trans. Faraday Soc.*, 1956, **52**, 261; (*b*) L. S. Lerman, *J. Mol. Biol.*, 1961, **3**, 18; (*c*) D. M. Bassini, J. Wirz, R. Hochstrasser and W. Leupin, *J. Photochem. Photobiol., A*, 1996, **100**, 65; (*d*) K. Fukui and K. Tanaka, *Nucleic Acids Res.*, 1996, **24**, 3962; (*e*) K. Fukui, M. Morimoto, H. Segawa, K. Tanaka and T. Shimidzu, *Bioconjugate Chem.*, 1996, **7**, 349; (*f*) A. I. Kononov, E. B. Moroshkina, N. V. Tkachenko and H. Lemmetyinen, *J. Phys. Chem. B*, 2001, **105**, 535; (*g*) S. Hess, W. B. Davis, A. A. Voityk, N. Rösch, M. E. Michel-Beyerle, N. P. Ernsting, S. A. Kovalenko and J. L. Pérez Lustres, *ChemPhysChem*, 2002, 1439; (*h*) J. Joseph, N. V. Eldho and D. Ramaiah, *Chem Eur. J.*, 2003, **9**, 5926.

9 M.-P. Teulade-Fichou, J.-P. Vigneron and J.-M. Lehn, *J. Chem. Soc., Perkin Trans. 2*, 1996, 2169.

10 (*a*) H. M. Gajiwala and R. Zand, *Macromolecules*, 1995, **28**, 481; (*b*) R. D. Patil and H. M. Gajiwala, *Polymer*, 1995, **38**, 4557; (*c*) S. Xu, M. Yang, J. Wang, H. Ye and X. Liu, *Synth. Metals*, 2003, **132**, 145.

11 (*a*) A. Elangovan, T.-Y. Chen, C.-Y. Chen and T.-I. Ho, *Chem. Commun.*, 2003, 2146; (*b*) C.-Y. Chen, J.-H. Ho, S.-L. Wang and T.-I. Ho, *Photochem. Photobiol. Sci.*, 2003, **2**, 1232; (*c*) A. Elangovan, S.-W. Yang, J.-H. Lin, K.-M. Kao and T.-I. Ho, *Org. Biomol. Chem.*, 2004, **2**, 1597; (*d*) F.-C. Chen, J.-H. Ho, C.-Y. Chen, Y. O. Su and T.-I. Ho, *J. Electroanal. Chem.*, 2001, **499**, 17.

12 G. D. Jaycox, G. W. Gribble and M. P. Hacker, *J. Heterocycl. Chem.*, 1987, **24**, 1405.

13 G. A. Reynolds and K. H. Drexhage, *Opt. Commun.*, 1975, **13**, 222.

14 (*a*) A. Elangovan, Y.-H. Wang and T.-I. Ho, *Org. Lett.*, 2003, **5**, 1841; (*b*) K. Sonogashira, Y. Tohda and N. Hagihara, *Tetrahedron Lett.*, 1975, **16**, 4467.

15 L. R. Faulkner, H. Tachikawa and A. J. Bard, *J. Am. Chem. Soc.*, 1972, **94**, 691.

16 Crystal data for **6**: formula $C_{23}H_{18}N_2$; formula weight: 322.39; unit cell parameters with standard deviations, cell length *a*: 9.2827(2) Å; cell length *b*: 9.3930(2) Å; cell length *c*: 10.7357(3) Å; cell angle *a*: 81.7260 (10)°; cell angle *β*: 72.9830 (10)°; cell angle *γ*: 71.801 (2)°; cell volume: 849.25(3) Å^3; symmetry space group: *P*$\bar{1}$; cell formula units *Z*: 2; temperature of study: 295(2) K; absorption coefficient: 0.02(2) mm^{-1}; reflections collected: 5997; independent reflections: 3827 (R_{int} = 0.0192); final *R* indices [$I > 2\sigma(I)$]: *R*1 = 0.0483, w*R*2 = 0.1278; *R* indices (all data): *R*1 = 0.0671, w*R*2 = 0.1449.